ALMA MEMO 379

SUMMER CLIMATE OVER CHAJNANTOR

Ricardo Bustos

Avda. Francesa 292, Concepción, Chile

Email: rbustos@dgf.uchile.cl

Abstract: A description of the main characteristics of the Bolivian High and what is now called the South American Monsoon System (SAMS) is presented. The water origin for the Altiplano can be inferred from both descriptions, being this supply mostly from the Amazon basin. From this premise, an analysis of ground weather station data and radiometers data from Chajnantor was performed.

During a summer event of high PWV, an anomalous increase of easterly winds is observed, confirming the previous "Amazon origin" assumption.

A summer climatology for Chajnantor is obtained and a daily index of U wind and PWV is defined. Both indexes present a high negative correlation during summer when U wind is negative. An *event* of high PWV during summer is also defined and a very significant contrast with a *no event* day is found. A composite analysis (averages) is done presenting the behaviour of PWV, winds, and temperature before, during, and after an *event* and a *no event* day.

These results produce a significant progress in the characterization of summer events of high PWV, its origin, and the planning for the implementation of future local weather forecasts.

1. Introduction

Recent studies have confirmed the existence of what is now called South American Monsoon System (SAMS). Its knowledge can provide very useful elements to improve the understanding of the climate in the Chajnantor area.

Uncertainties concerning the “monsoon climate” of South America still remain and the role of SASM in the global climate is even less known. For example, whereas the Asian monsoon is known to play a significant role in interannual variability such as El Niño Southern Oscillation, the influences of these fluctuations on SASM and possible feedback are virtually unknown. SAMS variability is closely linked to trade wind fluctuations over the equatorial Atlantic, which have significant impact on air-sea interaction related to ENSO as well as interannual and interdecadal sea surface temperature (SST) variations over the Atlantic.

During austral summer a warm-core anticyclone, known as the Bolivian high, strongly develops in the upper-troposphere over the Altiplano Plateau along with a tropospheric increase of temperature from the surface and capped by a cold top.

These summer-time variabilities, specially the tropospheric precipitable water vapour (PWV) content, are of interest for ALMA.

In this work, a summary of climatological summer features for the Altiplano is described and the empirical relations for Chajnantor are obtained, from site characterisation data.

Chapter 2 describes the existence of upper-level anticyclones around the world and focuses on the Bolivian high over South America. The influence of the Andes Mountains in the generation of the Bolivian high and its consequences over the Altiplano plateau are also described.

In Chapter 3, a summary of the South American Monsoon System (SAMS) is shown. A general view of the onset, mature phase, and demise of SAMS is described. A clear daily and annual cycle of SAMS is also described.

Chapter 4 focuses on rainfall variability and its effects over the Altiplano. A general view of the effects of El Niño Southern Oscillation (ENSO) to the Altiplano is described.

Chapter 5 analyses data from a weather station and measurements at 225 GHz and 183 GHz at Chajnantor and links the results with the previous chapters. A relation between zonal wind and precipitable water vapour during summer months is obtained.

Finally, conclusions on the effects of SAMS over the Altiplano and on the results obtained at Chajnantor are described in Chapter 6.

2. The Bolivian High

2.1 Upper-level anticyclones

Upper-tropospheric stationary waves represent some of the most distinct climatological features of the earth's atmosphere and are a consequence of inhomogeneities at the surface of the earth (land-sea contrast, orography, etc) observed throughout the globe and over a wide range of length scales. Of the many types of upper-tropospheric stationary patterns observed in the atmosphere, some of the most well-defined are found in the Tropics and subtropics in the form of closed anticyclones. At least four regions of closed anticyclonic circulation appears in 200 mb circulation (Figure 2.1) in both seasons, typically three or four in the summer hemisphere and one in the winter. For July, these regions are northwestern Mexico, the Arabian Gulf, the Tibetan highlands, and the western Pacific (around 10ºS), while in January the regions are Bolivia, southern Africa, northern Australia, and the western Pacific (near 15ºN and 10ºS).

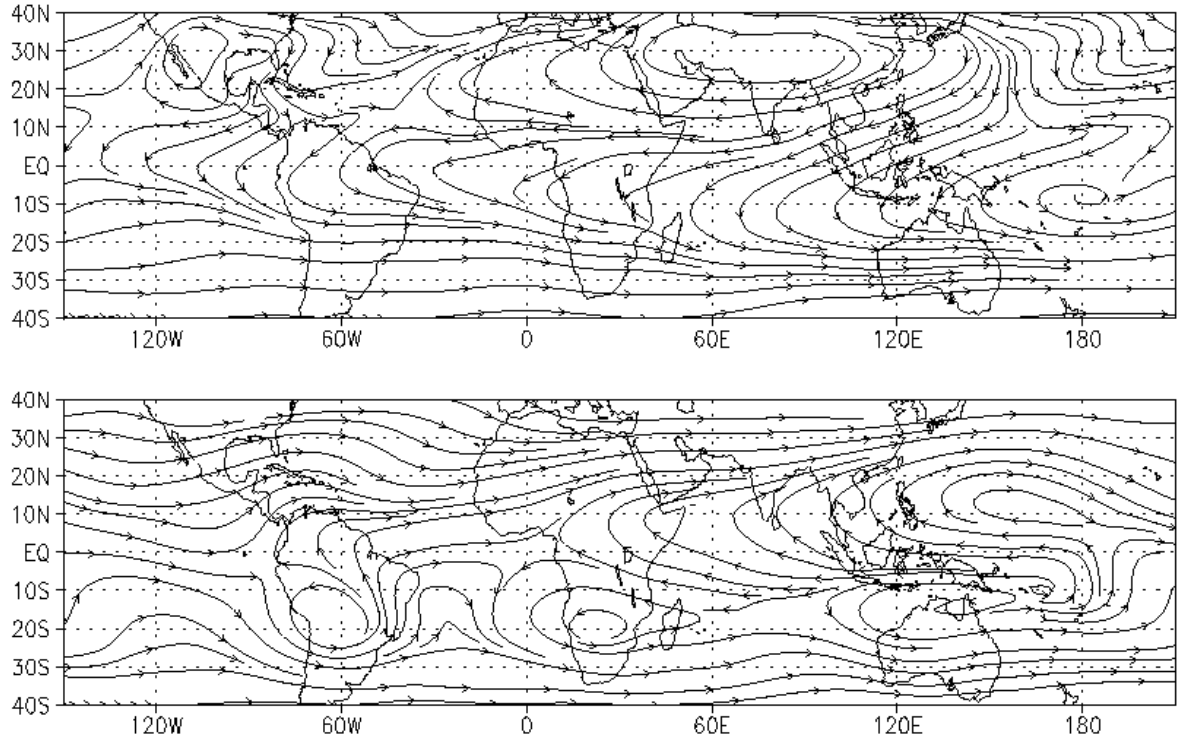

Figure 2.1: a) Climatological streamlines at 200 mb for July. b) as in a) but for January (from NCEP/NCAR).

Each of these upper-level anticyclones denotes a region of high pressure, accompanied in many cases by a trough (low pressure) to the east. It is generally recognized that upper-level highs such as these are part of a class of thermally induced features that form in regions of high precipitation in response to condensational heating, often representing an upper-level manifestation of the region's summer monsoon (Hastenrath 1991). As modelled by Matsuno (1966), Webster (1972), and Gill (1980), upper-level high pressure develops as a direct, linear response to imposed midtropospheric heating. However, not all upper-level tropical anticyclones fit the previous models, like the high in the Arabian Gulf, located at a considerable distance from the nearest region of high precipitation.

It is interesting to note that of the nine high-pressure cells shown in Figure 2.1, five are near high topography. This suggest that topography may play a role in the formation of some of these highs, either directly (through sensible heating or obstruction of the flow) or indirectly (e.g., by modifying the precipitation field). It is widely accepted that the Tibetan Plateau exerts a significant influence on the Asian summer monsoon and the upper-level Tibetan high. (Flohn 1968; Hahn and Manabe 1975; Zheng and Liou 1986). In South America, the effects of the Andes on the Bolivian high has received moderate attention yet remain an unresolved issue.

2.2 The Bolivian High

At 200 mb level, the Bolivian high in the NASA/DAO climatological data is positioned near 19ºS and 60ºW (Figure 2.2.a). Anticyclonic flow about the high is evident, with winds nearly parallel to the height contours except to the immediate west of the high and north of about 10ºS. Easterlies extend to the north of the Bolivian high, with a maximum wind speed of about 6 m/s occurring at 12º S. A deep trough to the east of the high is also observed in Figure 2.2.a, a feature that actually forms a closed low.

In Figure 2.2.b, a vertical cross section of the Bolivian high is presented, averaged from 10ºS to 25ºS, along with eddy temperatures (deviations from the zonal mean). As noted before by Kreuels et al (1975), the Bolivian high is characterized by a warm core below about 150 mb, capped above by a cold top. The warm temperatures extend from the surface and maximize at around 300 mb. Correspondingly, the geopotential anomaly is positive above 500 mb, with a maximum between 150 and 200 mb. The low pressure to the east (Nordeste low) has opposite characteristics, with a cold core and warm top.

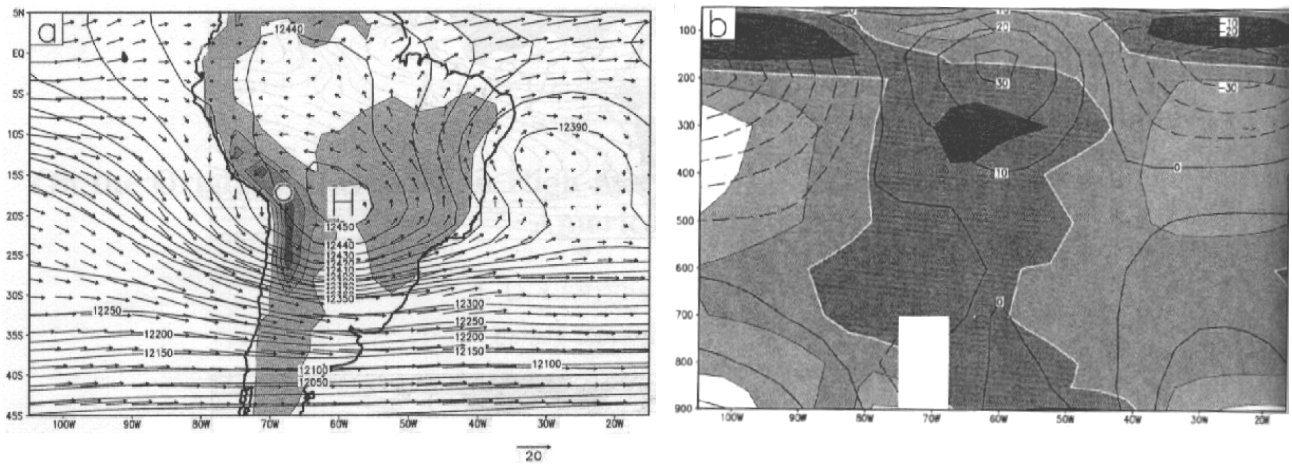

Figure 2.2: a) Geopotential height (maximum denoted by "H") and wind vectors at 200 mb from NASA/DAO observations. Above 12 350 m the contour interval is 10 m, while below it is 50 m. Shading denotes topography (contour interval 1000 m, starting at 250 m), and the vector in the lower right corner indicates a wind speed of 20 m/s. The approximate location of the Altiplano is shown with a white circle. B) Vertical cross section of anomalous geopotential height (contour interval 10 m, negative contours dashed) and anomalous temperature (shaded, 1 K interval; white contour denotes the 0 K line and darker shading denotes higher temperature), averaged from 10º to 25 ºS. (Lenters and Cook 1997)

According to Lenters and Cook (1997), the upper-tropospheric divergence over the Amazon that is balanced by equatorward flow south of the divergence maximum and high

pressure to the west can explain the positioning of the Bolivian high to the southwest of the Amazon basin. The positioning of the high's warm core is explained by the presence of compensatory subsidence off the subtropical west coast of South America. The adiabatic warming of this subsidence in the presence of westerly flow forms a warm anomaly to the east of the subsidence. In a similar fashion, the layer of cold air above the Bolivian high forms west of the precipitation in association with large-scale convective overshooting above the Amazon basin. This adiabatic cooling is embedded in easterly flow, thereby placing the cold layer to the west of the overshooting.

The Bolivian high is intimately related to other features of the South America climate. Numerous observational studies have noted a relationship between the seasonal variation in South American rainfall and the position and intensity of the Bolivian high. It is also recognized that the Bolivian high and the Nordeste low are dynamically linked (Kreuels et al 1975; Horel et al. 1989) and that the low is associated with sinking motion and the dry climate of northeast Brazil. Furthermore, the Bolivian high and Nordeste low may be related to convection and cold frontal penetrations associated with the South Atlantic Convergence Zone (SACZ). The position of the Bolivian high has also been related to interannual variability of precipitation on the Bolivian-Peruvian Altiplano. Aceituno and Montecinos (1993) have also noted a relationship between the Bolivian high and the episodic nature of summer precipitation on the Altiplano; during wet days the Bolivian high is more intense and displaced farther south than during dry days. From radiosondes, they also found negative (positive) U wind anomalies at Lima and Antofagasta at 500 mb during wet (dry) periods and that mid-tropospheric temperature (levels 700-300 mb) at Antofagasta and Quintero are considerably larger during the wet periods as compared with the dry ones.

2.3 Influence of the Andes

Lenters and Cook (1997) used a linear 30-level Global Circulation Model (GCM) to generate a realistic simulation of the Bolivian high and the associated circulation. Their GCM reproduced a reasonable structure in the wind, temperature and heating fields over South America. They found that most of the structure in the upper-tropospheric summer circulation is associated with condensational heating and that the Bolivian high represents a response to precipitation in the Amazon, Central Andes, and SACZ, with its position over the Altiplano being largely the result of Amazonian precipitation to the northeast, and its strength most strongly influenced by precipitation rates in the Central Andes.

An interesting GCM experiment without the Andean topography was done and much of the structure was reproduced in the absence of the Andes. They found that the only direct, mechanical effect of the Andes mountains on the upper-level circulation is a weak dynamic trough in midlatitudes. Sensible heating over the Altiplano generates a shallow monsoonal circulation that has little direct impact on the upper-tropospheric circulation. On the other hand, the Andes indirectly strengthen the Bolivian high by inducing precipitation in the central Andes and modifying precipitation elsewhere. However, the role of topography remains secondary, as evidenced by the presence of a well-defined Bolivian high in the absence of the Andes. The Nordeste low was successfully simulated by GCM as a direct, linear response to condensational heating considering the significance of remote precipitation, in particular African precipitation is required in conjunction with Amazonian precipitation to form a deep trough to the east of the Bolivian high.

3. South American Monsoon System (SAMS)

3.1 Description

As is described by Zhou and Lau (1998), monsoon climate is notable in many places around the world. The term “monsoon” usually indicates a seasonal reversal in the large-scale circulation system driven by differential heating of the continents and the oceans. According to Ramage (1971), South America is monsoonles since there is no seasonal reversal of wind direction in the lower troposphere over the region attributed to two primary reasons: 1) the narrowness of the continent away from the equator, which limits the areas in which heat lows can form, and 2) the persistent oceanic upwelling along the west coast, which keeps sea surface temperature lower than the continent all the year round. However, this notion of a monsoonles climate over South America lasted until the recent decade when the thermal impact of the Altiplano Plateau was brought into light (Rao and Erdogan 1989). Over the tropical Atlantic, the seasonal reversal of the surface wind is not readily apparent because the easterly trade winds prevail all year round. However, when the annual mean component is removed, the seasonal reversal in surface winds becomes evident (Figure 3.1).

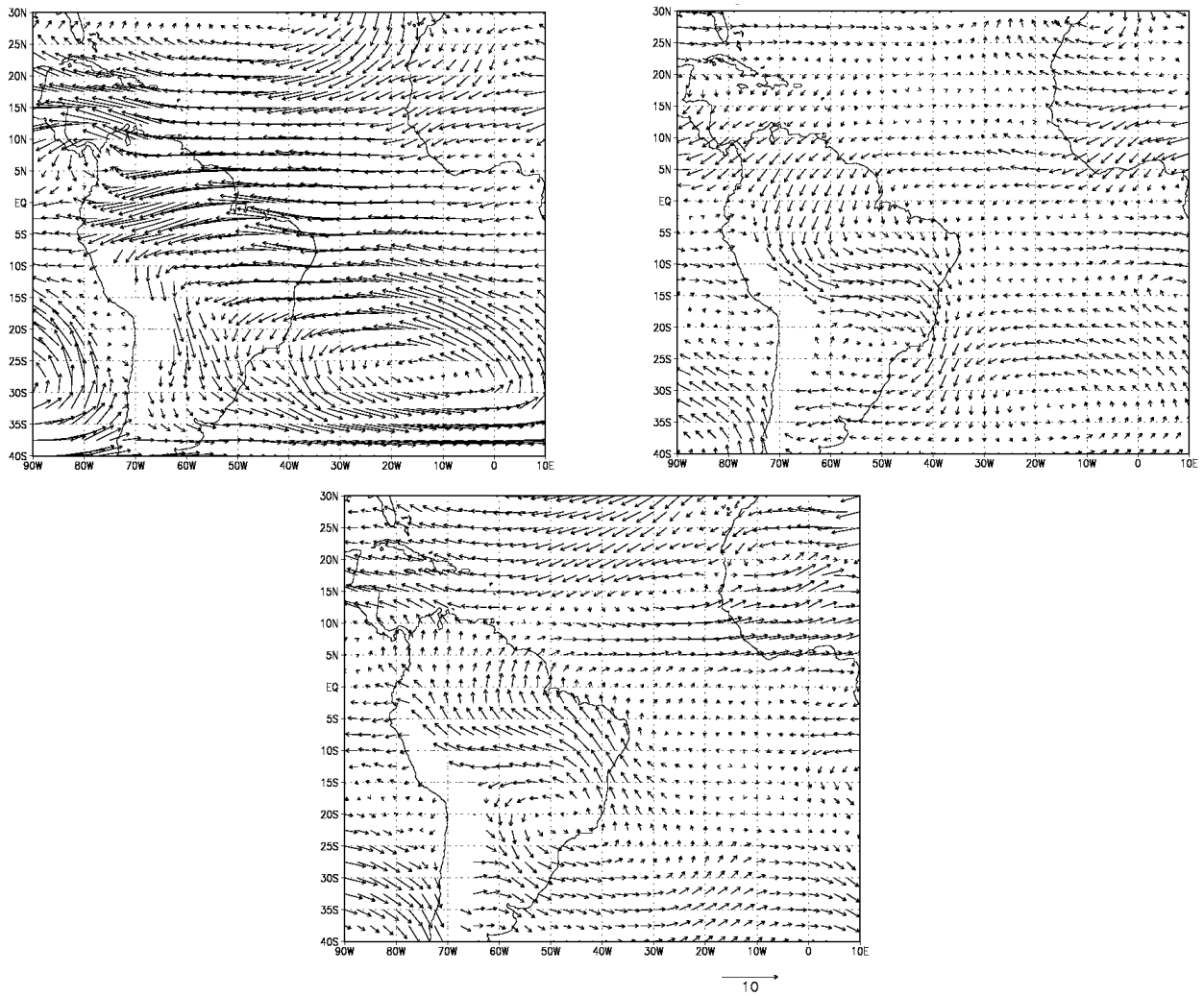

Figure 3.1 NCEP/NCAR climatology of 850 mb wind (m/s) for a) annual mean; b) January minus annual mean; c) July minus annual mean.

In the Southern Hemisphere summer, the anomaly flow originates from the Subsaharan region and substantially enhances the Tropical North Atlantic easterly trades. After crossing the equator, it becomes a northwesterly flow along the eastern side of the Andes, then turns clockwise around the low of Gran Chaco. Clearly, this flow reverses its direction in southern winter. The above noted reversal wind is one of the many factors of a monsoon climate in South America.

A warm-core anticyclone known as the Bolivian high strongly develops in the upper-troposphere over the Altiplano plateau of Peru and Bolivia (15ºS - 21ºS). Located to the east is an upper-level trough extending over the western South Atlantic. Meanwhile, a continental heat low develops at low levels in the region of the Paraguayan-Argentinean Gran Chaco and Pampean Sierras. Distinct northerly and northwesterly low-level flow evolves along the eastern slopes of the tropical and subtropical Andes and east-northeasterly trades prevail over much of the Amazon basin.

Lenters and Cook (1995) identified five climatological summertime precipitation maxima over South America in January. They found that the precipitation maxima in the Amazon, South Atlantic Convergence Zone (SACZ), and northern Andes regions are mostly the results of low-altitude continental heating. The precipitation maxima over the eastern flank of central Andes and the western flank of the southern Andes are introduced by the barrier effect of the mountain. Strong precipitation at high elevations of Central Andes is associated with locally driven small-scale convergence, which may be related to the strong sensible and latent heating over the Altiplano Plateau.

3.2 Annual cycle of SAMS

The climate of tropical and subtropical South America is characterized by a regular and pronounced annual cycle in rainfall. Austral summer (December, January, and February; DJF) is the rainy season for a large portion of the central region of South America, whereas austral winter (June, July, and August; JJA) is the dry season. Some parts of South America, such as Colombia, southern Venezuela, norhtwestern Brazil, and some regions of southern South America do not experience a dry season and, therefore do not have a well defined rainy season. From the northwestern parts of South America to central and southeastern Brazil, the rainfall season changes progressively from JJA to DJF, following the annual migration of the deep tropical convection and the establishment of a heat low in central South America in summer.

A pentad outgoing longwave radiation (OLR) climatology for South America displays considerable seasonal variation of deep convection over Central and South America (Figure 3.2). OLR data is used as a proxy of cloudiness (Bustos 2001).

For most of South America between the equator and 20ºS there are distinct dry and wet seasons each year. These correspond approximately to the southern winter and summer seasons respectively. The onset of the rainy season begins in the western Amazon basin in late August. Deep convection and rainfall, as represented by OLR values less than 220 W/m^2, shifts southward along the east slopes of the Andes, and southeastward towards the Brazilian highland during September and October (Figure 3.2.a). By late November, deep convection covers most of western South America from the equator south to 20ºS, while there is a noticeable absence of

deep convection over the eastern Amazon basin and northeast Brazil. Throughout this period the deep convection, associated with Intertropical Convergence Zone (ITCZ), is confined to the central Atlantic between 5ºN and 8ºN.

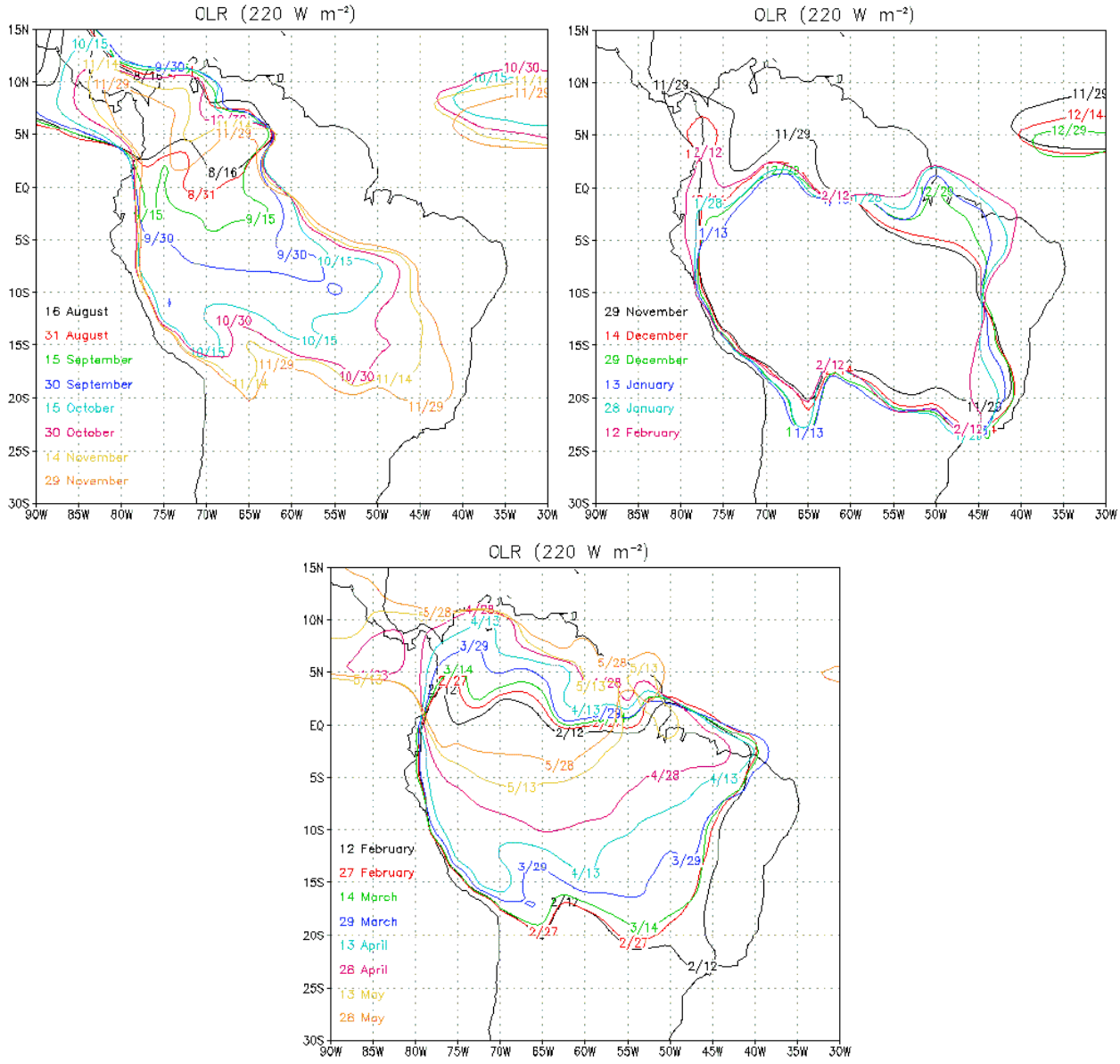

Figure 3.2. The 1979-1995 mean evolution of the 220 W/m^2 contour of OLR for the period a) 16 August - 29 November; b) 29 November - 12 February; c) 12 February - 28 May. Analysis is based on the pentad climatology, available from the Climate Prediction Center, Washington, DC. (Grimm and Garreaud 1998)

From late November through mid-February (Figure 3.2.b), the mature phase of the South American Monsoon System, there is little change in the areal extent of the deep convection, except over the eastern Amazon basin, which gradually experiences an increase in deep convection throughout the period. As deep convection spreads into the eastern Amazon, deep convection associated with the Atlantic ITCZ weakens.

Beginning in March, the South American Monsoon System begins to weaken as the area of deep convection retreats northwestward, especially over central and western sections (Figure 3.2.c). However, deep convection over the north coastal regions of Brazil doesn't begin to weaken until late April. Throughout the demise phase of SAMS deep convection associated with the Atlantic ITCZ remains relatively weak.

During austral summer, latent heat released from deep cumulus convection over these regions of intense rainfall dominates the total diabatic heating over South America. The diabatic heating is maximum in the middle and upper troposphere over the Altiplano and the southern Amazon basin.

Sensible heat flux near the surface constitutes an additional heat source of the SAMS. Sensible heating dominates the lower troposphere and it reaches its maximum strength before the onset of the Monsoon, when the spring-to-summer increment of surface insolation over the subtropical latitudes is redistributed to the troposphere by dry, shallow convection. The interaction between these two heat sources and the tropospheric circulation is essential in shaping the climatological SAMS.

The seasonal migration of the ITCZ in the eastern tropical Pacific and Atlantic does not follow the apparent trajectory of the sun, which crosses the equator twice a year. In October, sea surface temperatures at and to the south of the equator are low, and the ITCZ is farthest north. That is not the case over the continents, where the maximum cloudiness is near the equator. During the subsequent months, the continental convective zones move southward, but over the waters of the eastern Pacific and Atlantic, the ITCZ remains in a northerly position. By April, the waters south of the equator have warmed, and the ITCZ moves toward the equator. In the Pacific it only reaches the equator while over the Atlantic, it reaches as far as 10ºS, near the Brazilian coast. In this last region, the ITCZ remains slightly south of the equator from February through April.

4. Summer rainfall over the Altiplano

4.1 Description

The only water resource over this semiarid region is virtually during the summertime rainfall. A major fraction of the summer rainfall and snowmelting represent the only recharge of the underground water system of the Altiplano and the dry western slope of the Andes. Surface heating and deep moist convection release large amounts of energy into the middle and upper troposphere over the central Andes linking rainfall variability on the Altiplano with circulation and rainfall anomalies over the rest of South America. Over 60% of the annual precipitation is concentrated in the austral summer (DJF) in the form of intensive convective rainstorms along the plateau, when easterly flow prevails over the central Andes allowing moisture transport from the interior of the continent up to the Altiplano. Rainy days tends to cluster in 'rainy episodes', lasting from 1 to 2 weeks, interrupted by dry periods of similar length. Despite high daily solar radiation receipts throughout the summer months, precipitation occurs in discrete episodes rather than a constant process (Aceituno and Montecinos 1993).

Aceituno and Montecinos (1993) were able to show that precipitation amounts on the Altiplano were significantly higher when the Bolivian High was intensified and displaced south of its climatological position. This displacement of the High to the south of the Altiplano leads to an enhanced easterly flow on its northern side and increased moisture flux from the interior of the continent toward the Altiplano. On the other hand, dry periods over the Altiplano are normally related to either upper air convergence or strong westerly flow.

Vuille et al (1998) describes that moisture advection is most pronounced near the 500 mb level and is accompanied by easterly winds in the surface and midtropospheric layers. This moisture input, however, reduces with increasing distance from the water vapour source, which lies in the tropical lowlands to the east. As a result, precipitation amounts decrease from E to W across the Altiplano.

4.2 Diurnal cycle of precipitation

Convective cloudiness exhibits a well-defined diurnal cycle tied to the solar radiation. During the rainy season, there is a preference for an afternoon / evening maximum of deep convection over continental areas, since the land surface heating tends to destabilize the lower troposphere. Nevertheless, Garreaud and Wallace (1997) demonstrated that the timing of the maximum convection is more location-dependent and closely linked to regional topographic features such as mountain ranges and concave coastlines. The maximum of convection during evening is very pronounced over the central Andes, along the northeast coast of the continent, and in two parallel bands over southern Amazonia. On the other hand, convection tends to peak during late night and early morning along the eastern slope of the central Andes, over the subtropical plains, and off the northeast coast of the continent.

4.3 Interannual variability

Several studies have shown a weak relationship between ENSO and summertime rainfall that could be at least partially caused by the large spatial and intraseasonal variability of the precipitation over the Altiplano. Vuille et al. (2000) shows that ENSO-related rainfall anomalies are much more pronounced over the western sector compared with those over the northeastern sector of the Altiplano. Garreaud and Aceituno (2001) have noted that previous studies relating ENSO and Altiplano interannual rainfall anomalies can be explained by the generalized warming (cooling) of the tropical troposphere during the warm (cold) phase of ENSO, and the associated changes in the seasonal mean zonal flow aloft at tropical-subtropical latitudes. In any case, the physical link between global-scale circulation anomalies and Altiplano rainfall anomalies is unclear (Garreaud and Aceituno 2001).

Fluctuations in rainfall on the Altiplano exhibit an easterly/wet - westerly/dry relationship. The amount of the Altiplano rainfall anomalies is highly dependent on the location of zonal wind anomalies. Thus, seasonal prediction in this region requires detailed knowledge of the structure of the tropical-subtropical tropospheric circulation anomalies (Garreaud and Aceituno 2001).

It is also important to notice that during austral winter (JJA), a direct relation between ENSO and wet anomalies of PWV was found (Bustos et al 2000). Though amounts of precipitable water vapour during JJA are significantly smaller than in summer months, they show interannual variability more related to the ENSO phenomenon, with wet (dry) winter anomalies coinciding with El Niño (La Niña) events.

5. Observations at Chajnantor

5.1 Data

The meteorological data is obtained from a weather station functioning in Chajnantor since April 1995 and providing data every 10 minutes approximately. Temperature, wind speed, and wind direction data are used in this work.

Observations of precipitable water vapour (PWV) from 1995 to 2000 are derived from opacity (τ) measurements from a 225 GHz tipping radiometer maintained by NRAO in Chajnantor. The 225 GHz opacity, τ, is obtained every 10 minutes approximately (McKinnon 1987). This value, based on measurements done with a 183 GHz radiometer (Delgado et al, 1999), is converted in PWV by:

$$PWV = -0.052088 + 20.876\tau$$

PWV observations for 2001 are directly obtained from a 183 GHz radiometer.

In all datasets, the data obtained every 10 minutes was averaged to obtain a one-hour average.

The atmospheric data used in this work is available at the NRAO web page, maintained by Simon Radford (http://www.tuc.nrao.edu/mma/sites/Chajnantor/data.c.html).

5.2 Daily and annual cycles

The previous chapters described a very pronounced rainfall season on the Altiplano during austral summer months. A seasonal reversal of winds produced in South America during these months lead to moisture input over the Altiplano from the Amazon basin in a seasonal easterly flow. As is seen on figure 5.1, daily and annual cycles of zonal wind (U wind) and temperatures are evident. On the x-axis days from 1995 to 2001 are represented while in the y-axis daily hours in UTC are represented. Precipitable water vapour also exhibits an annual cycle, but daily cycle during summer is not evident due to high PWV events (Figure 5.1.c). It is clearly seen in figure 5.1.a that easterly flow is present during summer months and during nighttime and early morning (5 - 15 UTC, 2 - 12 local time).

Interannual variability in easterly flow is also seen. Summer of 1996 has a lower easterly flow while in the summers of 1997 and 2001 an increase of easterly flow is observed.

Easterly flux near the surface also produces an increase of night and early morning temperatures as is seen on figure 5.1.b. During summer of 1996, almost no easterly flow was observed and night temperatures were lower than the other summers.

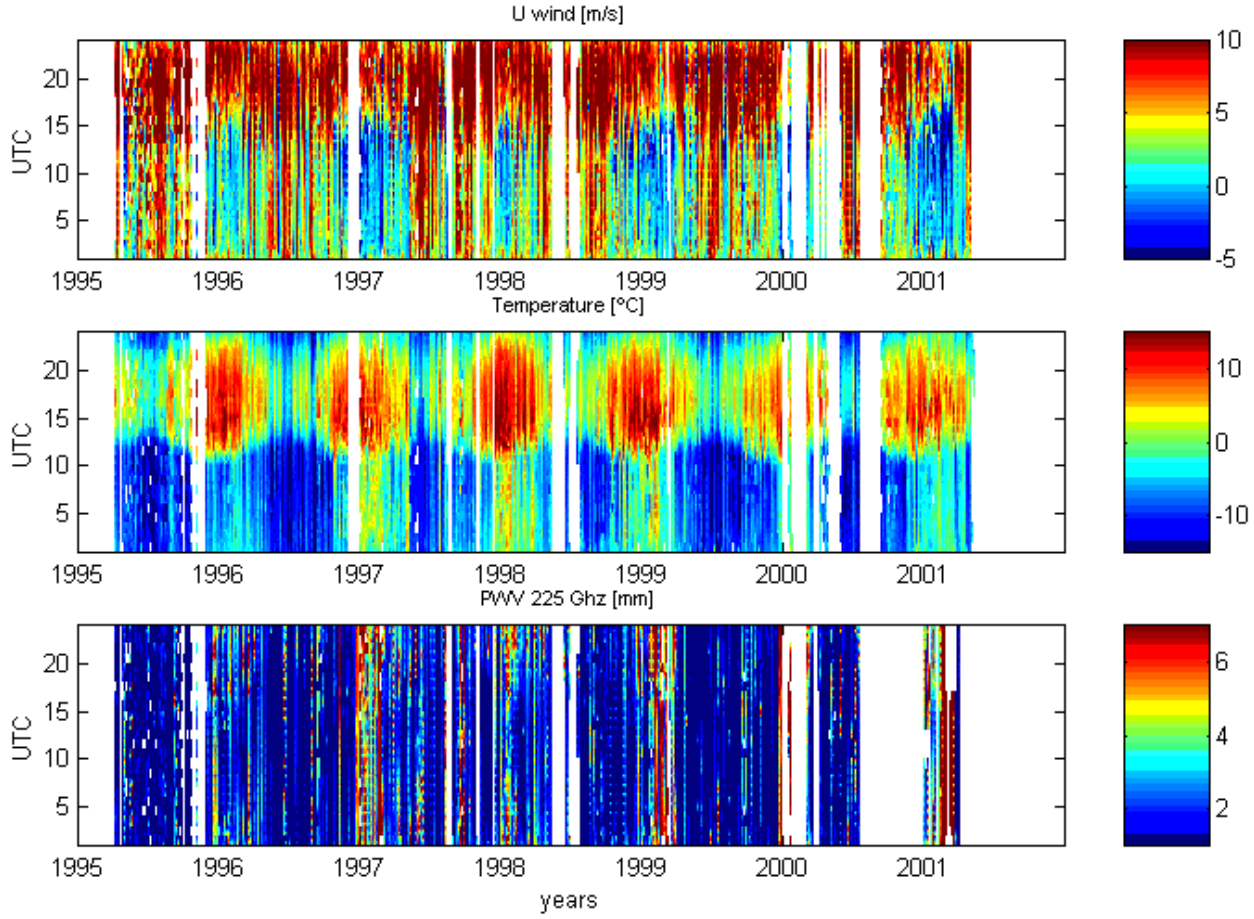

Figure 5.1: a) U wind, b) temperature, c) PWV measured at Chajnantor. The x-axis are days from 1995 to 2001 and the y-axis are daily hours in UTC.

5.3 Climatological summer daily cycle

On figure 5.2, summer daily cycles of U wind, V wind (meridional wind), and PWV are shown. This situation is an average and can be considered as summer climatology, not a "normal" day. These cycles are averages from December 15 to March 15 from 1995 to 2001. A clear daily cycle of U and V wind is seen. During a climatological summer day in Chajnantor, at the beginning of the night (1 UTC, 10 PM local time) a decrease of wind speed, mostly southwesterlies is perceived and changes to a weak northwest breeze. Then, a relative calm during the night is observed until 8 UTC (5 AM local time), when wind direction is turned to an easterly flow with a moderate northerly flow. This easterly flow maximises at 13 UTC (10 AM local time) and begins to weaken until 15 UTC (12 AM local time) when an increase of wind speed is observed with a change in direction. A west south-west wind maximises at 21 UTC (6 PM local time) and decrease again until midnight.

In contrast, PWV daily cycle has a moderate behaviour compared with winds, with a minimum during early hours and an increase of moisture from 14 UTC (11 AM local time) until 1 UTC (10 PM local time). This is relevant to determine the origin of the water source. When the easterly flow begins in early morning, the atmospheric column is filled with water vapour

reaching a maxima after noon. A delay of 6 hours is observed between the time when easterly flow begins and the increase of PWV. However, a detailed analysis of this situation with radiosonde data can lead to a better understanding on how this evolves during the day, especially for the presence of a morning inversion layer capping the Chajnantor area (G. Delgado, personal communication).

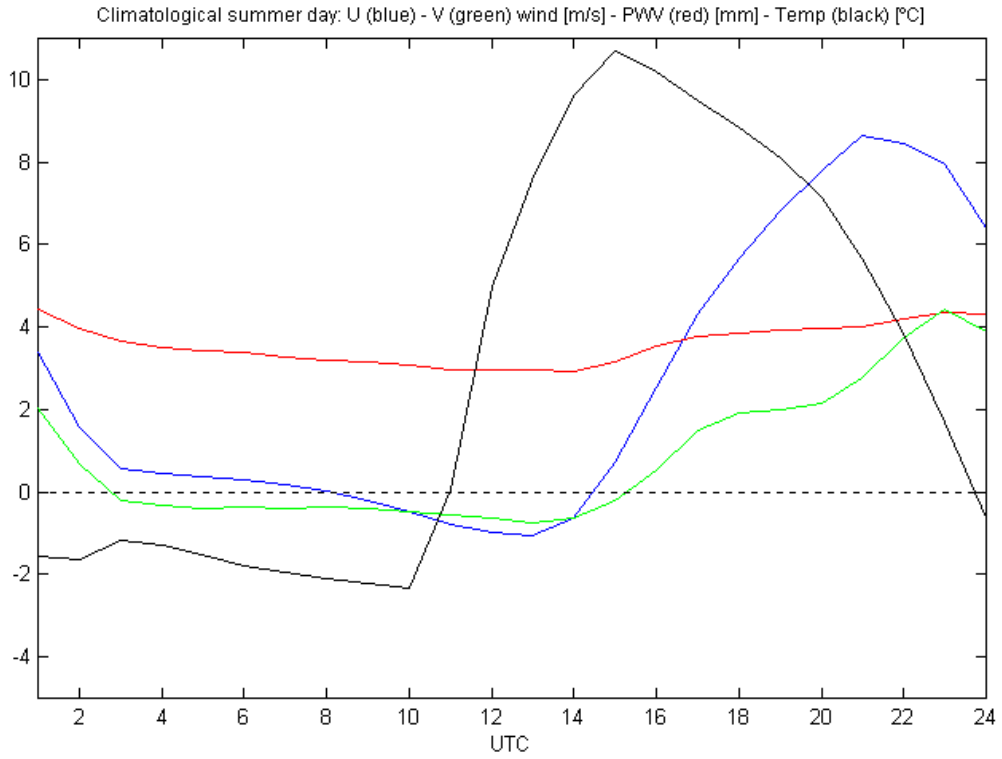

Figure 5.2: Daily cycle of U (blue) and V (green) wind, PWV (red), and temperature (black). Averages are from December 15 to March 15 of years 1995 to 2001.

From figure 5.2, it is clearly seen that easterly wind blows from 8 to 14 UTC. A daily index that accounts for the amount of easterly winds in one day is the average of U wind within these hours. Early morning and afternoon winds are not considered on this average to avoid the influence of westerly winds. The daily index of U wind is named in this work: *8-14 UTC U wind*.

In the same way, in order to have a daily index in the amount of PWV, averages from 14 to 24 UTC of PWV are considered. This also avoids the influence of low values of PWV before noon on this average. The daily index for PWV is named in this work: *14-24 UTC PWV*.

5.4 U wind - PWV Summer relation

During summer months, easterly flow becomes an important factor in the increasing moisture over Chajnantor, as is seen on figure 5.3.a. It is also important to notice that during winter, north-west wind direction prevails (Figure 5.3.b). However, during summer this situation changes when meridional winds almost disappear and the easterly flow becomes the dominant wind direction.

Precipitable water vapour has very low values during winter, with averages less than 1 mm per month. In summer, this changes to averages of more than 6 mm. This increase in PWV is due to the increase of the easterly flow that transports moisture from the Amazon basin.

Intraseasonal variability of PWV connected with variability of easterly winds becomes evident as is seen on figure 5.3.b. During summers of 1996 and 1998, low values of PWV are coincident with low values of easterly winds. Summer of 1997, 1999, 2000 and 2001 exhibits high values of PWV, also coinciding with an increase of easterly winds.

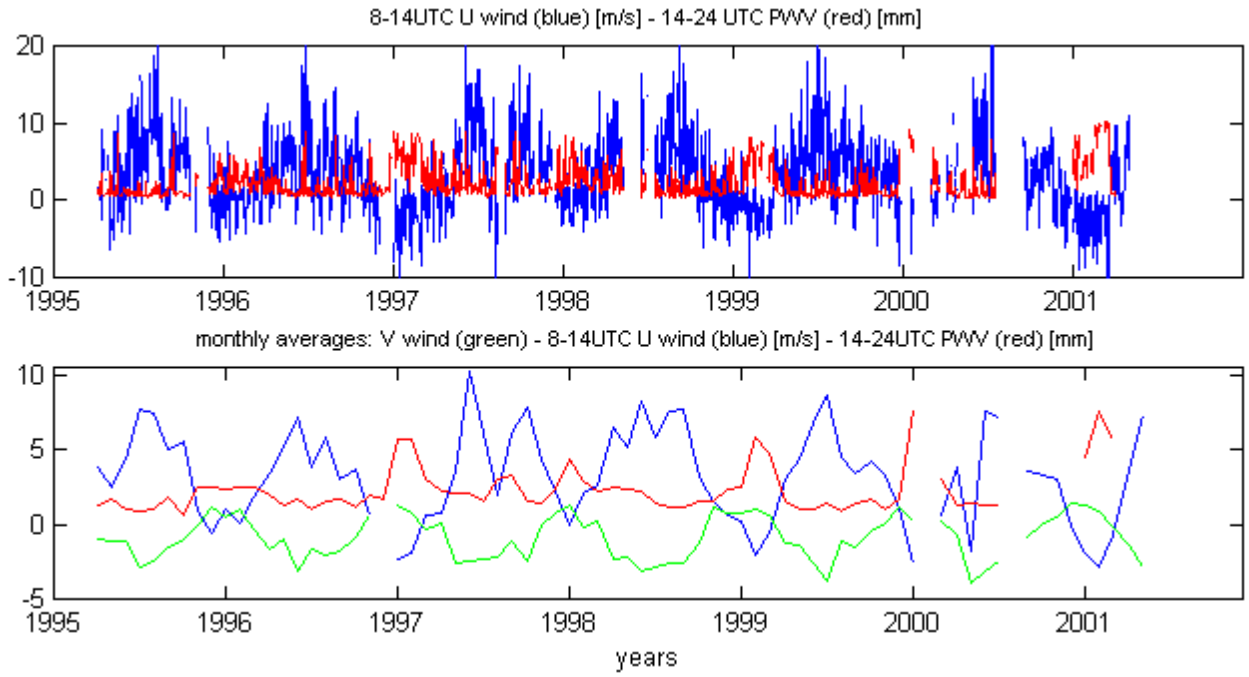

Figure 5.3: a) Daily *8-14 UTC U wind* (blue) and *14-24 UTC PWV* (red). b) Monthly averages of a) and monthly averages of daily V wind (green) are shown.

From the scatter diagram of monthly averages of *8-14 UTC U wind* and *14-24 UTC PWV* depicted on figure 5.4, two different zones can be defined. The first zone is associated with negative *8-14 UTC U wind*. A linear relation with *14-24 UTC PWV* is observed, with an increase of easterly winds producing an increase in the amount of PWV. Performing a cross-correlation analysis for this zone, eliminating one 'spurious' element, a value of –0.7595 is obtained.

The other zone is associated with positive *8-14 UTC U wind*. In this zone, *14-24 UTC PWV* is independent to the increase of westerly winds. Increase of westerly wind, that drags dry air from the Atacama Desert, does not produce significant changes in the amount of PWV that remains with low values.

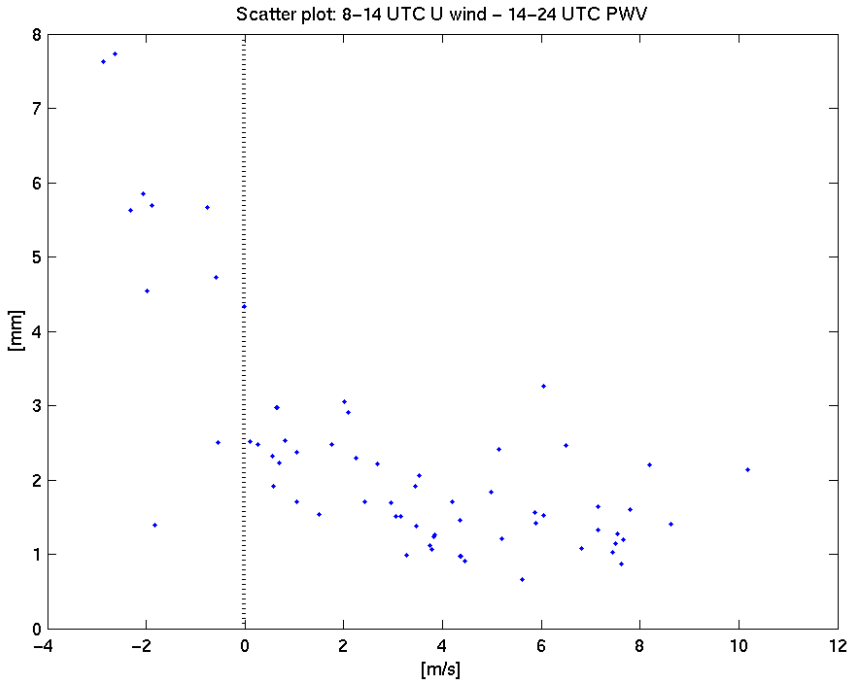

Figure 5.4: Scatter diagram of monthly averages of *8-14 UTC U wind* and *14-24 UTC PWV*.

Figure 5.5 shows summer anomalies of *8-14 UTC U wind* and *14-24 UTC PWV* during 1995 to 2001. During summer, different events of high amounts of PWV occurred in discrete periods ranging from 2 to 7 days as is seen on the next figures. During this episodes of high PWV (red positive anomalies) it is seen that anomalous easterly winds (blue) previously occurs.

During January and February of 1996 (Figure 5.5.a), positive anomalies of *8-14 UTC U wind* indicates a decrease of easterly winds. In this period, most of the *14-24 UTC PWV* anomalies are negative. In general, this summer presented low values of easterly winds and low values of PWV.

Some events of high amounts of *14-24 UTC PWV* in short periods (3 - 7 days) are observed in late December of 1996 and during January and February of 1997 (Figure 5.5.b). An inverse relation with easterly flow is evident during these events.

In summer of 1998, three events of high *14-24 UTC PWV* are shown on figure 5.5.c. One in December of 1997, with a period of 4 days. Easterly flow is not present during this event but the day before did. In early January of 1998, another event of 4 days is observed. In middle January of 1998, an event of high PWV of 7 days occurred. In these last two cases, easterly flow was higher than as usual.

Summer of 1999 (figure 5.5.d) presented several events of high *14-24 UTC PWV* and easterly winds prevailed in these cases.

In the summer of 2000 (figure 5.5.e), two events are observed but the lack of data in January and February does not give a general view of that summer.

In the summer of 2001 (figure 5.5.f), an unusual long event of high *14-24 UTC PWV* is observed from middle February to middle March. Easterly winds prevailed during this one-month period.

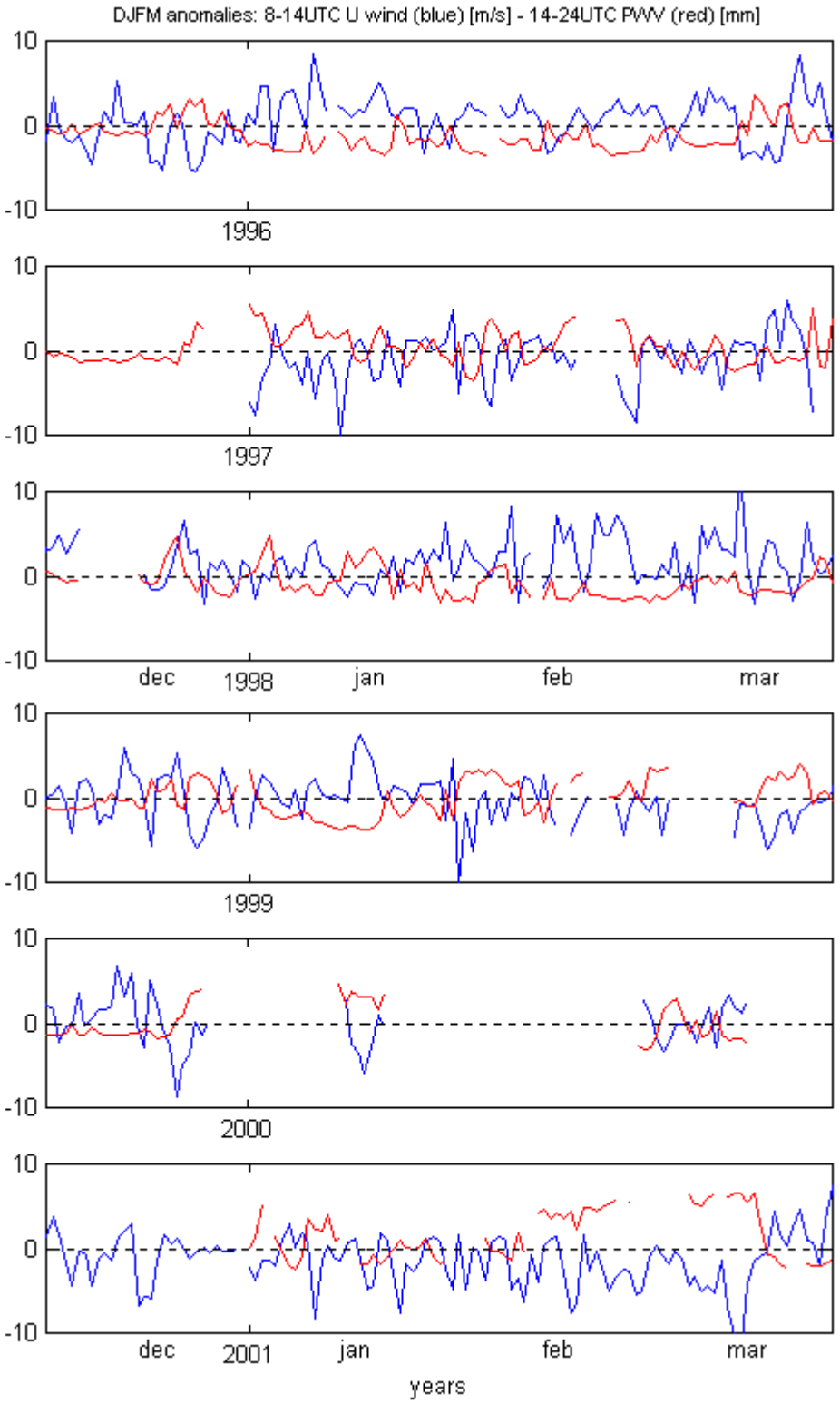

Figure 5.5: Summertime series (DJFM, Dec-Jan-Feb-Mar) from 1995 to 2001 of daily *8-14 UTC U wind* and *14-24 UTC PWV*. a) 1996, b) 1997, c) 1998, d) 1999, e)2000, and f)2001.

5.5 Summer events of high PWV

From the total number of days during summer (from Dec. 15 to Mar. 15) 20% of the days with larger average PWV values are selected. These days can be considered as a poor event for radioastronomical observation. In order to have the 20% criterion, 86 *events* of the available 431 days (there are 111 summer days with no data) with a daily average over 5.9 mm are selected. The other 80% with PWV daily average lower than or equal to 5.9 mm are considered as a *no event* day. This occurs in 345 days of 431 available days.

The PWV daily average for *event* days is 7.47 mm while the PWV daily average for *no event* days is 2.84 mm.

An average daily cycle for these days of *events* and *no events* can then be plotted as on figure 5.6. This figure gives very interesting aspects of the climate when an event of high PWV occurs. The dotted line corresponds to a *no event* day.

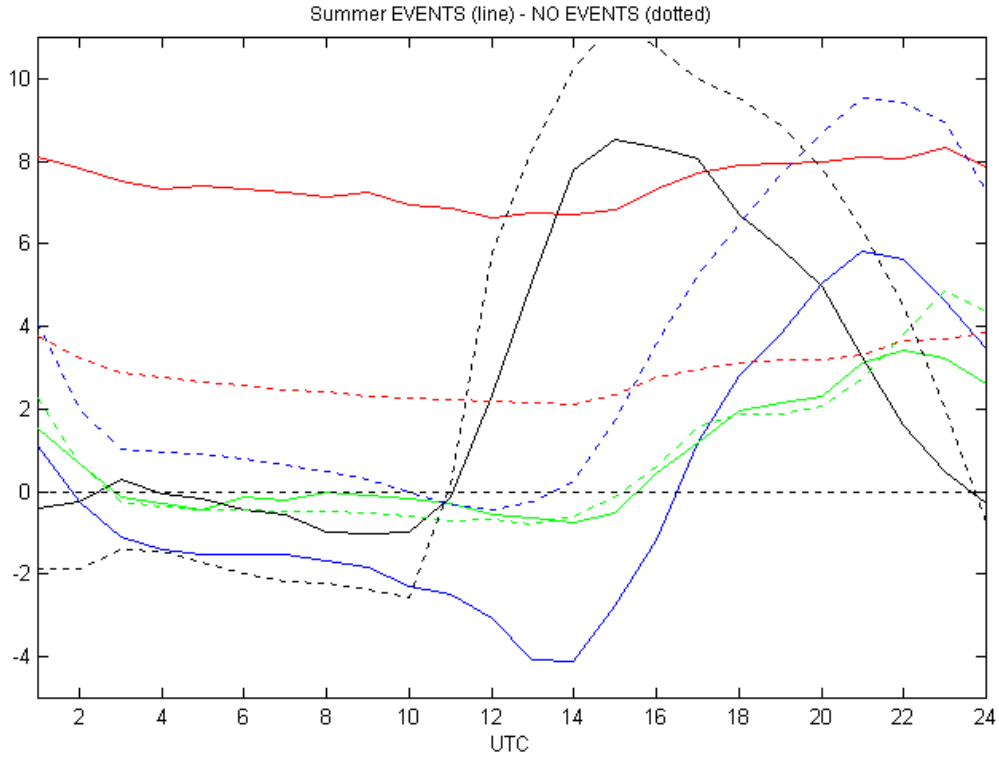

Figure 5.6: Daily average of summer *events* (line) and *no events* (dotted). U (blue) and V (green) wind, PWV (red), and temperature (black)

It is very interesting to notice the increase of easterlies during an *event*. Easterlies begin near local midnight at Chajnantor (2 UTC), peaks at 14 UTC (11 AM local time), and then changes to a westerly direction at 17 UTC (2 PM local time). This contrast with a *no event* day also proves that the moisture input to the Chajnantor area is from the east. This difference is very significant since a weak easterly is observed in a *no event* day, while 14 consecutive hours of negative U wind are blowing in a day of high PWV. We must keep in mind that a *no event* day occurs in 80% of summer days.

Meridional wind during these *events* is not a factor that affects the increase of moisture, since the difference from a *no event* day is negligible. Therefore, only the increase of negative U wind controls the increase of PWV over Chajnantor as is clearly seen from figure 5.6.

Also, during the *event* days night temperatures are warmer in 1.5ºC than during a *no event* day, as more humidity coming from the east is present in the air. During daytime, temperatures are lower during *event* days than during *no event* days probably due to the formation of cloudiness or the occurrence of rain and storms that reduce solar radiation to the surface.

The average daily cycle evolution of PWV during an *event* does not present significant changes and is only biased in 4.63 mm compared with a *no event* day.

5.6 Composites

Averages of *event* and *no event* days can be done to obtain composites. For the case of a *no event* composite, an "8-day window" of continuous *no event* days is chosen for the average, being the day in the middle of this window the selected day named 0. From the total of summer days, 33 "8-day window" are selected and averaged. Figure 5.7 shows the results of this average. The day 0 and the previous days do not present eastern flow. A clear daily cycle of PWV that varies from 2 to 4 mm can be seen. Due to the definition of the "8-day window", the days after day 0 slightly increase the easterly wind because in some cases, the day 5 corresponds to an *event* day.

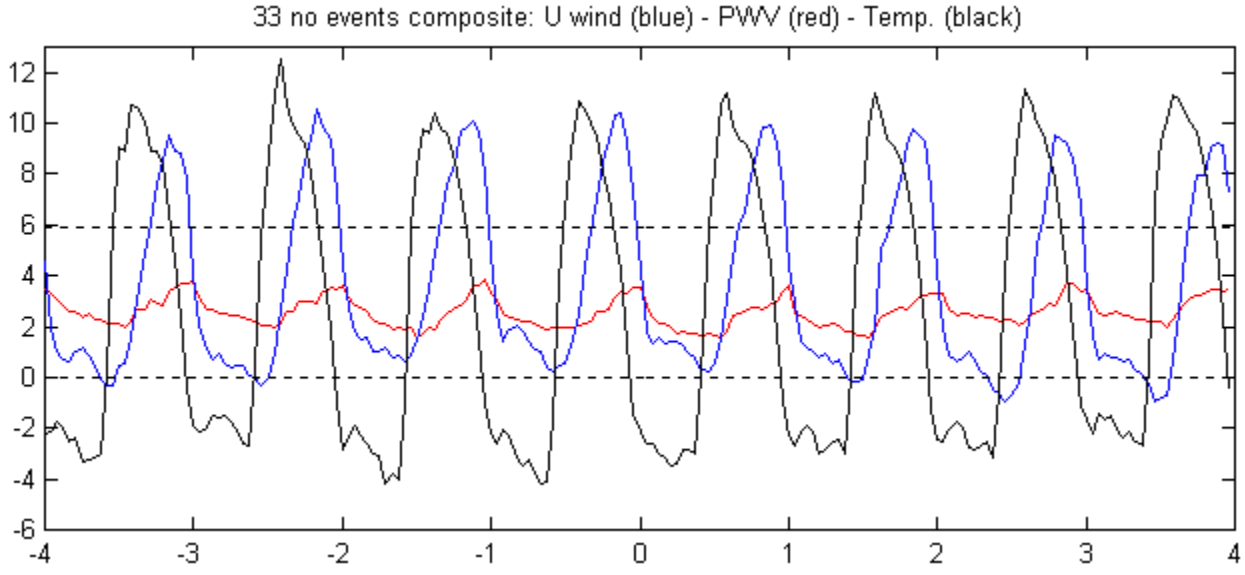

Figure 5.7: Composite of a *no event* day. Dotted line represents the threshold value of 5.9 mm.

A composite of *event* days is also obtained. In this case the days when the *event* begins ("day 0") has to be found. For the total period, 18 "days 0" are selected for the average. The negative days corresponds to the averages of the days previous to the *event* to occur and the positive days, the average of days after the *event* has occurred, that in some cases are still events (*events* extend from 1 - 5 day approximately). Figure 5.8 shows how PWV increases from 4 mm (day -2) to be over 5.9 mm during an *event* (remember that the definition of an event is when the PWV daily average is over 5.9 mm). It is very interesting to notice the increase of easterly winds the day before the *event*. The day -4 and -3 have a very similar behaviour than the day 3 of figure 5.7, so changes are detected 2 days before the *event,* when a slightly increase of PWV and night temperatures are observed. Daily temperature decreases during an *event*. Although some of these results were also found in the previous section (5.5), the behaviour of the days previous to the *event* is very significant to observe and has to be considered for the future planning of forecasts of *events* in Chajnantor.

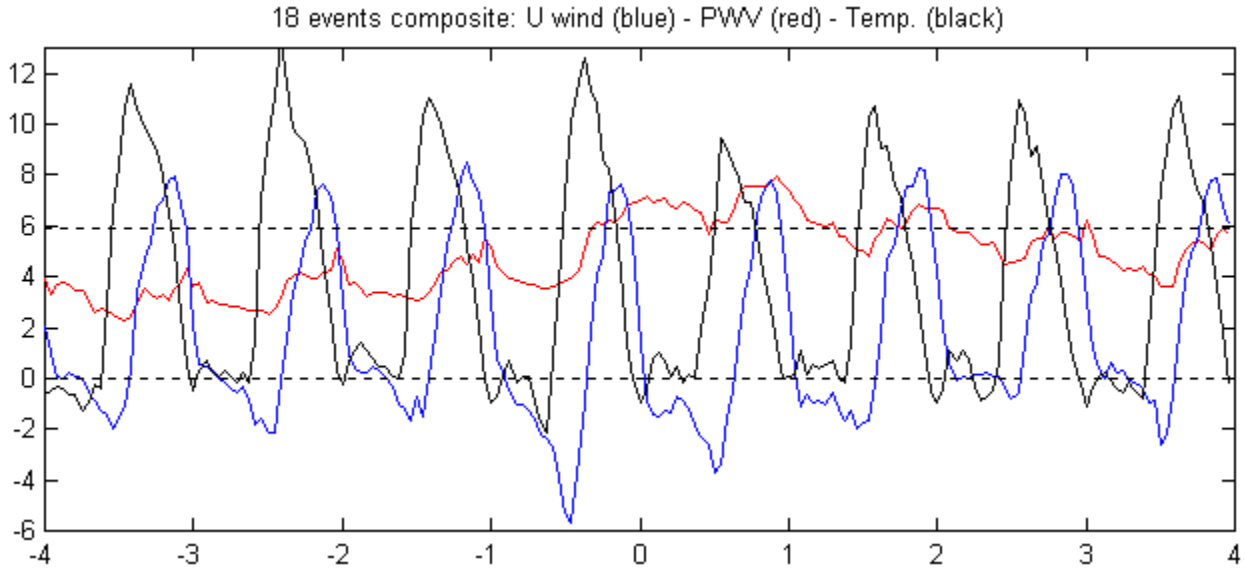

Figure 5.8: Composite of an *event* day. Dotted line represents the threshold value of 5.9 mm.

6. Conclusions and future work

Summer climate over the Altiplano is modulated by the existence of the Bolivian high generated by the South American Monsoon System. Its knowledge is very important to understand the climate variability over Chajnantor and can provide very useful elements for the operation planning of a future large array radiotelescope.

Theoretically, the resource of water for the Altiplano is coming mainly from the Amazon basin and it is usually transported during night-time and early morning, when easterly winds prevail over the Altiplano. A direct relation between early morning easterly flow and afternoon increase of PWV is found, with easterly flow increase preceding the increase of PWV. Anomalous increase of easterly winds produces an anomalous increase of moisture that in some cases can produce rainfall episodes over the Altiplano.

As is seen on figure 5.2, climatological summer daily cycles of U wind, V wind, PWV and temperature are obtained. A relative calm during the night is observed until 8 UTC (5 AM local time), when wind direction is turned to an easterly flow with a moderate northerly flow. This easterly wind maximises at 13 UTC (10 AM local time) and weakens until 15 UTC (12 AM local time), when an increase of westerly flow is observed. PWV daily cycle has a moderate behaviour compared with winds, with a minimum during early hours and an increase of moisture from 14 UTC (11 AM local time) until 1 UTC (10 PM local time). A delay of 6 hours is observed from the beginning of the easterly flow to the increase of PWV.

In the case of negative U wind (easterly wind), the daily index defined for U wind and PWV presents a negative correlation (-0.7595). In the case of positive U wind (westerly wind), its increase does not produce significant changes in the amount of PWV that remains with low values as is seen on the scatter plot (figure 5.4).

Variability of PWV connected with variability of easterly winds becomes evident from the time series (figure 5.5) and daily cycles (figure 5.6). During summers of 1996 and 1998, low values of PWV are observed coinciding with low easterly winds. Summer of 1997, 1999, 2000 and 2001 exhibits high values of PWV, coinciding with increasing easterly winds.

In 86 *events*, representing the 20% of summer days with PWV daily averages larger than 5.9 mm, a huge increase of U winds during night-time and early morning is observed. A *no event* is considered the 80% summer days with PWV daily averages inferior to 5.9 mm. The U wind behaviour difference between an *event* and a *no event* day is enormous and confirms the predominant water origin from the Amazon basin from an increase of easterlies with the consequently increase of PWV. Therefore, easterly winds control the increase of PWV over Chajnantor during summer.

This easterly flow near the surface constitutes an additional heat source increasing night surface temperatures at Chajnantor. Due to the increase of PWV and the possible formation of cloudiness, a decrease in solar radiation to the surface decreases day-time temperatures during *event* days.

Daily cycle of PWV during *events* does not change significantly from *no event* days and the delay between the increase of easterlies and the increase of PWV must be studied in the

future. Analyses with radiosonde data can give more information about how these events evolve during the day.

The study of composites clearly shows strong easterly winds the day before and during *events* of high PWV. Comparing event days on a case-to-case study with the obtained composites will allow to define different "classes" of events. These "classes" can be associated to synoptic scales can be determined separating cases of rainfall, storms, cloudiness, and clear sky conditions with high amount of PWV. This study should be done to improve a future forecast of high PWV *events*.

Acknowledgements

Thanks are given to the Meteorology Section of the Department of Geophysics, University of Chile for the use of facilities and access to documentation.

Data from NRAO was obtained from the site characterisation page (http://www.tuc.nrao.edu/mma/sites/Chajnantor/data.c.html) maintained by Simon Radford. 183 GHz radiometer provided by Guillermo Delgado.

Thanks are also given to Dr. Guillermo Delgado (Onsala Space Observatory / European Southern Observatory) for the review of this manuscript and his constructive comments.

Glossary

Adiabatic process: A thermodynamic change of state of a system in which no heat or mass is transferred across the boundaries of the system. In an adiabatic process, compression always results in warming, and expansion in cooling. Vertical motions of air parcels in the atmosphere are approximately adiabatic.

Advection: Horizontal transport of an atmospheric property (e.g. temperature, moisture, or vorticity) solely by the wind.

Anticyclonic: Having a sense of rotation about the local vertical that is clockwise in the Northern Hemisphere and counterclockwise in the Southern Hemisphere. Opposite of cyclonic.

Convection: In meteorology, convection is generally applied to atmospheric motions that are predominantly vertical. It may refer to upward-motions.

El Niño/Southern Oscillation (ENSO): The term for the coupled ocean-atmosphere interactions in the tropical Pacific characterised by episodes of anomalous high sea surface temperatures in the equatorial and tropical eastern Pacific; associated with large-scale swings in surface air pressure between the western and eastern tropical Pacific. These episodes recur at irregularly spaced intervals (2-7 years) and may persist for as long as 2 years.

General Circulation Model (GCM): Numerical representation of the atmosphere and its phenomena over the entire earth, using the equations of motion and including radiation, photochemistry, and the transfer of heat, water vapour, and momentum.

Geopotential height: A measure of the altitude of a point in the atmosphere, expressed in terms of its potential energy per unit mass (geopotential) at this altitude relative to sea level. It is used in essentially all operational upper-air reports and charts.

Geostrophic wind: A hypothetical model describing an unaccelerate horizontal wind that blows in a straight path parallel to isobars or contours above the friction layer; it results from a balance between the horizontal components of the pressure gradient force and the Coriolis effect. In the Southern Hemisphere, the geostrophic wind is oriented such that lower (higher) pressure is to the right (left) of the wind.

Hadley cell: A direct thermally driven and zonally symmetric circulation first proposed by George Hadley (1685-1768), as an explanation for the trade winds. It is essentially closed circulation system, consisting of the equatorward movement of the trade winds between a latitude of about 30º and the equator in each hemisphere, with rising wind components near the equator, poleward flow aloft, and finally descending components at about 30º latitude again.

Intertropical Convergence Zone (ITCZ): A narrow, discontinuous belt of convective clouds and thunderstorms paralleling the equator and marking the convergence of the trade winds of the two hemispheres; this zone shifts seasonally.

Latent heat: The heat released or absorbed per unit mass by a system in a reversible, isobaric-isothermal phase change. In meteorology, the latent heats of vaporization (or condensation), fusion (or melting), and sublimation (or deposition) of water substance are of importance.

Meridional wind: The wind or wind component along the local longitude. The meridional wind component is positive if it blows from the south and negative if from the north.

Monsoon: Wind in the general atmospheric circulation, typified by a seasonal persistent wind direction and by a pronounced change in direction from one season to another. The term is generally confined to a situation where primary cause is the differential heating between a continent and the adjacent ocean.

Sea Surface Temperature (SST): Temperature of the surface layer of a body of water.

Sensible heat:The heat absorbed or transmitted by a substance during a change of temperature that is not accompanied by a change of state. It can be measured with a thermometer.

Streamline: The pattern of flow of air moving horizontally; on a map, lines that are drawn everywhere parallel to wind direction.

Subtropical high: One of the semipermanent anticyclones of the subtropical high pressure belt. They lie over oceans, and are best developed and displaced poleward in the summer season.

Subtropics: The indefinite belts in each hemisphere between the tropic and temperate zones. The poleward boundaries are considered to be roughly 35º N and S, but vary greatly according to continental influence.

Trade winds (or trades): The wind system, occupying most of the Tropics, which blows outward from the subtropical highs toward the equator trough; Surface winds are southeasterly in the Southern Hemisphere, known as southeast trades.

Trough: An elongated area of relatively low atmospheric pressure at a given level; usually an elongated area of cyclonic curvature of the wind field. Opposite of a ridge.

U wind: Zonal wind. Component of the wind in the west-east direction.

V wind: Meridional wind. Component of the wind in the north-south direction.

Vortex: Any circular flow possessing vorticity; more often it refers to a flow with closed streamlines.

Vorticity: Measure of the rotational spin about an axis at some point within a fluid. Although any orientation of the spin axis is possible, vertical vorticity component describing the rotation about a vertical axis is commonly used.

Zonal wind: The wind or wind component along the local parallel or latitude. The zonal wind component is positive if it blows from the west and negative if from the east.

References

Aceituno, P., and A. Montecinos, 1993: Circulation anomalies associated with dry and wet periods in the South American Altiplano. Preprints, *Proc. Fourth Int. Conf. On Southern Hemisphere Meteorology*, Hobart, Australia, Amer. Meteor. Soc., 330-331.

Bustos, R., G. Delgado, L. Nyman, and S. Radford, 2000: 52 years of climatological data for the Chajnantor area. ALMA Memo Series No. 333.

Bustos, R., 2001: OLR study for the Paranal and Chajnantor area. Internal report presented to the European Southern Observatory.

Delgado, G., A. Otárola, V. Belitsky, D. Urbain, and P. Martin-Cocher, 1999: The determination of precipitable water vapour at Llano de Chajnantor from observations of the 183 GHz water vapour line. ALMA Memo Series No. 271.

Flohn, H., 1968: Contributions to a meteorology of the Tibetan Highlands. Atmos. Sci. Paper 130, 120 pp. [Available from Colorado State University, Department of Atmospheric Science, Fort Collins, CO 80523.]

Garreaud, R., and J. Wallace,1997: The diurnal march of the convective cloudiness over the Americas. *Mon. Wea. Rev.*, **125**, 3157-3171.

Garreaud, R., and P. Aceituno, 2001: Interannual rainfall variability over the South American Altiplano. *J. Climate*, to be published.

Geer, I. W., 1996: *Glossary of Weather and Climate*. American Meteorology Society.

Grimm, A., and R. Garreaud, 1998: Report of the VAMOS working group on the SAMS. October 1998, Miami, Florida.
http://www.met.utah.edu/jnpaegle/research/miami_report.html.

Hahn, D. G., and S. Manabe, 1975: The role of mountains in the South Asian monsoon circulation. *J. Atmos. Sci.*, **32**, 1515-1541.

Hastenrath, S., 1991: *Climate Dynamics of the Tropics*. Kluwer. Academic Publishers, 488 pp.

Horel, J. D., A. N. Hahmann, and J. E. Geisler, 1989: An investigation of the annual cycle of convective activity over the tropical Americas. *J. Climate*, **2**, 1388-1403.

Kreuels, R., K. Fraedrich, and E. Ruprecht, 1975: An aerological climatology of South America. *Meteor. Rundsch.*, **28**, 17-24.

Lenters, J. D. and K. H. Cook, 1995: Simulation and diagnosis of the regional summertime precipitation climatology of South America. *J. Climate*, **8**, 2988-3005.

———, 1997: On the origin of the Bolivian high and related circulation features of the South American climate. *J. Atmos. Sci.* **54**, 656-677.

McKinnon, M., 1987: Measurement of atmospheric opacity due to water vapour at 225 GHz. ALMA Memo Series No. 40.

Ramage, C. S., 1971: *Monsoon Meteorology*. Academic Press, 269 pp.

Rao, G. V., and S. Erdogan, 1989: The atmospheric heat source over the Bolivian Plateau for a mean January. *Bound.-Layer Meteor.*, **46**, 13-33.

Vuille, M., et al, 1998: Atmospheric circulation anomalies associated with 1996/1997 summer precipitation events on Sajama Ice Cap, Bolivia. *J. Geophys. Res.*, **103**, 11,191-11,204.

Vuille, M., R. S. Bradley, and F. Keimig, 2000: Interannual climate variability in the Central Andes and its relation to tropical Pacific and Atlantic forcing. *J. Geophys. Res*, **105**, 12447-12460.

Zheng, Q., and K. N. Liou, 1986: Dynamic and thermodynamic influences of the Tibetan Plateau on the atmosphere in a general circulation model. *J. Atmos. Sci.*, **43**, 1340-1354.

Zhou, J., and K. M. Lau, 1998: Does a Monsoon climate exist over South America?. *J. Climate*, **11**, 1020-1040.